

Decay of Color Gauge Fields in Heavy Ion Collisions and Nielsen-Olesen Instability

Aiichi IWAZAKI

*International Politics and Economics, Nishogakusha University
2590 Ohi, Kashiwa, Chiba 277-8585, Japan*

We analyze the behavior of unstable modes in the glasma produced in high energy heavy ion collisions, using a simple model with effective homogeneous longitudinal color electric and magnetic fields. The unstable modes are approximately described as Nielsen-Olesen unstable modes under the homogeneous longitudinal gauge fields. We find that the Nielsen-Olesen unstable modes show properties very similar to those of the exponentially increasing unstable modes in the glasma recently shown by Romatschke and Venugopalan. Although initial gauge fields in the glasma are much stronger than the ones in our model, they decay with the production of the Nielsen-Olesen unstable modes. We discuss why we can reproduce the features of the glasma by using the effective homogeneous weak magnetic fields. Our analysis supports an idea that the decay of the gauge fields in the glasma is caused by Nielsen-Olesen instability.

§1. Introduction

In high energy collisions of heavy ions in RHIC or LHC, the most important ingredients for producing quark gluon plasma (QGP) are small x gluons in the nuclei.^{1)–5)} The small x gluons with also small transverse momenta are sufficiently dense in the nuclei and so they may be treated as classical fields produced by glassy large x gluons even after the collisions of the nuclei. It has been shown that longitudinal color magnetic and electric fields of the small x gluons are generated initially at the collisions. They are classical fields and evolve classically according to a color glass condensate (CGC) model.⁶⁾ These fields, which are called as glasma, are expected to give rise to QGP by their rapid decay.^{7),8)}

In an extremely high energy collision, the thickness of nuclei is nearly zero due to the Lorentz contraction. Thus, the initial gauge fields have only transverse momentum perpendicular to the collision axis, but have no longitudinal momentum (rapidity dependence). Such classical gauge fields can not possess any longitudinal momentum in their classical evolution, since equations of motion of the gauge fields are invariant under the Lorentz boost along the collision axis.^{2)–4)} Thus, the naive application of the CGC model, e.g. McLerran-Venugopalan model (MV model),⁶⁾ does not give rise to thermalized QGP. It has recently been shown,⁹⁾ however, that the addition of small fluctuations with rapidity, e.g. quantum fluctuations^{10),11)} to the initial gauge field induces exponentially increasing modes with longitudinal momentum. The production of the exponentially increasing modes implies that a process toward thermalization has started; the decay of the gauge field and the isotropization of momenta. Although the decay of the classical fields have been clarified in the numerical calculations, the physical mechanism of the decay is still unclear.

In this paper we show using a simple model of an initial gauge field that the decay of the glasma is caused by Nielsen-Olesen unstable modes.^{(8), (12)–(14)} The modes arise under the initial gauge field when small fluctuations around the gauge fields are taken into account. Especially we compare the time evolutions of the unstable modes with those of the exponentially increasing modes of longitudinal pressure shown in the previous calculation.⁽⁹⁾ We find that the previous main results can be reproduced.

The initial gauge field in our model is spatially homogeneous and much weaker than the fields of the glasma.⁽⁹⁾ The glasma are strong (e.g. color magnetic field $B \sim O(Q_s^2/g)$) and inhomogeneous (their coherent length being the order of $\sim Q_s^{-1}$; Q_s is a saturation momentum written as $Q_s = g^2\mu$ in the ref.⁽⁹⁾) The initial gauge field is chosen to reproduce the time evolutions of the instabilities observed in the reference.⁽⁹⁾ It can not reproduce local behaviors of the instabilities in the transverse space since it is homogeneous in the space.

Nielsen-Olesen instability is associated with color magnetic fields, not color electric fields. In the paper we are only concerned with the instability of the color magnetic fields. The color electric fields produced in heavy ion collisions are unstable against quark pair creations⁽¹⁵⁾ so that they may decay sufficiently fast. We do not discuss the instability of the color electric fields.

In the next section, we explain the instabilities observed in the previous simulation.⁽⁹⁾ In the section(3), we review briefly Nielsen-Olesen instability. In the section(4), we explain the assumption used in our model, especially the relevance of the use of homogeneous color magnetic field instead of inhomogeneous glasma. In the section(5), we introduce our simple model for analyzing the decay of the glasma in τ and η coordinates. In the section(6), we compare our results with those obtained in the previous simulation.⁽⁹⁾ In the final section, we conclude our results.

§2. Instabilities in initial gauge fields

In high energy heavy ion collisions, classical color gauge fields are generated and are pointed to the collision axis (longitudinal direction). They are color electric and magnetic fields. They arise at $\tau = 0$ just when the collisions occur. (Here we assume collisions in high energy limit where heavy ions are Lorentz contracted to have zero width. Thus, the collisions occur at the instance of $\tau = 0$; $\tau = \sqrt{x_0^2 - x_3^2}$.) They have sufficiently large energy densities to produce thermalized quark gluon plasma in the subsequent their decay. The color gauge fields are coherent states of small x gluons with transverse momenta less than a saturation momentum, Q_s . These gluons are described by a model of color glass condensate, e.g. MV model. More explicitly, the color gauge fields are given initially at $\tau = 0$ as functions of color charge density of large x gluons inside of heavy ions; the color charge density is determined with a Gaussian distribution in the MV model.

Such classical gauge fields are uniform in the longitudinal direction. On the other hand, they are not uniform in the transverse directions; the scales of their variations in the directions are typically determined by the saturation momentum Q_s . This is because they are made of the gluons possessing transverse momenta typically given by Q_s . This implies that the fields keep their directions (parallel

or anti-parallel to the collision axis) inside of transverse regions whose widths are given typically by Q_s^{-1} . But, they change their sign outside of the region. In this way their directions are never uniform in the transverse directions, although they are uniform in the longitudinal direction.

Anyway, such color gauge fields are given initially in the collisions. After their production they evolve according to the gauge field equations. Since the gauge fields equations are invariant under Lorentz boost along the collision axis denoted by x_3 ($\eta = \log(\frac{x_0+x_3}{x_0-x_3}) \rightarrow \eta + \text{cont.}$), the color gauge fields have no dependence of η in their development. That is, the gauge fields are still uniform in the longitudinal direction after the collision. In such a circumstance, a numerical calculation⁵⁾ has been performed to show that they evolve smoothly in time τ and become weak owing to their expansion. Any unstable behaviors of the fields were not found in the calculation. Non-linearity in the gauge field equations seems not to play dramatic roles in the evolution of the gauge fields. Actually, it has been shown¹⁴⁾ that their time developments can be reproduced qualitatively in the linear analysis of the field equations; especially the fields become weak with time as $1/\tau$. (A kind of "Abelian dominance"¹⁶⁾ seems to hold for large τ since self-interactions of gauge fields become ineffective because of smallness of the fields in the large τ .) We use the feature in order to make our simple analytical model of the glasma decay.

Subsequently, a numerical simulation has been performed⁹⁾ with a slightly modified initial condition. That is, much small gauge fields depending on η are added by hand to the original initial gauge fields. Such gauge fields may arise because the uniformness in η of the initial condition is broken in real situations: Heavy ion collisions occur with finite energies or the initial conditions derived in the MV model receive high order quantum corrections. Both of them give rise to much small corrections depending on η to the initial gauge fields without η dependence.

The simulation has clarified the existence of unstable modes in the evolution of the gauge fields; Fourier components in η of longitudinal pressure increase exponentially in τ . This implies that a component of gauge fields added in the simulation increases exponentially. The existence of the modes implies that the initial color electric and magnetic fields uniform in the longitudinal direction are unstable under the small fluctuations depending on η .

We should note that since gauge field fluctuations depending on η are sufficiently smaller than the initial gauge fields, they can be treated perturbatively. That is, the fluctuations evolve under the background initial gauge fields without self-interactions. Hence, the analysis of their evolution can be performed in the linear approximation.

Here, we review characteristic properties of the unstable modes found in the numerical simulation. We denote the longitudinal pressure as P_η . When we denote Fourier components as $P_\eta(k_\eta, \tau) = \int d\eta P_\eta(\eta, \tau) \exp(ik_\eta\eta)$ (k_η denotes longitudinal momentum), $P_\eta(k_\eta, \tau)$ evolves smoothly in τ when initial gauge fields have no dependence of the rapidity η . Obviously, $P_\eta(k_\eta, \tau) \propto \delta(k_\eta)$ in the case. Once gauge fields depending on η are added to the initial gauge fields, $P_\eta(k_\eta, \tau)$ shows exponential increase. Namely some unstable modes are excited when gauge fields fluctuations depending on η are added. $P_\eta(k_\eta, \tau)$ shows the exponential increase just after a time

$\tau(k_\eta) > 0$ passes. In other words, $P_\eta(k_\eta, \tau)$ does not increase exponentially until the time $\tau = \tau(k_\eta)$. The simulation shows that $\tau(k_\eta) \propto k_\eta$. That is, the component $P_\eta(\tau, k_\eta)$ begins to increase exponentially later than the time when components $P_\eta(\tau, k'_\eta)$ ($k'_\eta < k_\eta$) increase. Hence, we can define a maximum momentum $k_\eta(\text{max})$ at the instance τ such that the component $P_\eta(\tau, k_\eta(\text{max}))$ begins to increase exponentially at the instance; components $P_\eta(\tau, k_\eta < k_\eta(\text{max}))$ have already increased exponentially. The simulation shows that $k_\eta(\text{max})$ increases linearly with time τ .

Another interesting property found in the simulation is concerned with longitudinal momentum distribution at a time τ , namely $P_\eta(k_\eta, \tau)$. The distribution has a peak at the value of $k_\eta(p)$, which is almost independent of τ . This implies that the unstable modes with the characteristic longitudinal momentum $k_\eta(p)$ are induced dominantly. The peak in the distribution, $P_\eta(k_\eta(p), \tau)$, increases such as $P_\eta(k_\eta(p), \tau) \propto \exp(\text{const} \cdot \tau^{1/2})$.

We should mention that the growth rate of the peak is much smaller than the typical time scale Q_s^{-1} in the system. Thus, it takes a too long time for the small gauge field fluctuations to become comparable order of magnitude of the initial gauge fields. This is a bad new for the realization of thermalized QGP through the decay of the gauge fields.

We will show that these characteristic properties can be understood using Nielsen-Olesen instability. The point in our analysis is that the background initial gauge fields are approximately described by Abelian gauge fields and the gauge field fluctuations added can be treated perturbatively. Based on the approximation, we show that the unstable modes found in the numerical simulation are just Nielsen-Olesen unstable modes.

§3. Nielsen-Olesen Instability

We review briefly Nielsen-Olesen instability by using SU(2) gauge theory. The instability means that homogeneous color magnetic field is unstable in the gauge theory. In order to explain it, we decompose the gluon's Lagrangian with the use of the variables, "electromagnetic field" $A_\mu = A_\mu^3$, and "charged vector field" $\Phi_\mu = (A_\mu^1 + iA_\mu^2)/\sqrt{2}$ where indices $1 \sim 3$ denote color components,

$$L = -\frac{1}{4}\vec{F}_{\mu\nu}^2 = -\frac{1}{4}(\partial_\mu A_\nu - \partial_\nu A_\mu)^2 - \frac{1}{2}|D_\mu\Phi_\nu - D_\nu\Phi_\mu|^2 - \\ + ie(\partial_\mu A_\nu - \partial_\nu A_\mu)\Phi_\mu^\dagger\Phi_\nu + \frac{g^2}{4}(\Phi_\mu\Phi_\nu^\dagger - \Phi_\nu\Phi_\mu^\dagger)^2 \quad (1)$$

with $D_\mu = \partial_\mu + igA_\mu$, where we have omitted a gauge term $D_\mu\Phi_\mu = 0$.

We can see that the charged vector fields Φ_μ couple with electromagnetic field A_μ minimally through the covariant derivative D_μ and non-minimally through the interaction term, $ig(\partial_\mu A_\nu - \partial_\nu A_\mu)\Phi_\mu^\dagger\Phi_\nu$. When a homogeneous color magnetic field $B > 0$ described by $A_\mu = A_\mu^B$ is present, we analyze the fluctuations Φ_μ under the color magnetic field. To do so, we solve the following equation of Φ under the background field B ,

$$(\partial_t^2 - \vec{D}^2 \mp 2gB)\phi_{\pm} = 0 \quad (2)$$

with $A_j^B = (-Bx_2, Bx_1, 0)/2$, where $\phi_{\pm} = (\Phi_1 \pm i\Phi_2)/\sqrt{2}$ and $\vec{D} = \vec{\partial} + ig\vec{A}^B$. Index \pm denotes a spin component parallel (+) and anti-parallel (-) to $\vec{B} = (0, 0, B)$. We have assumed the magnetic field pointed into x_3 direction. In the equation, higher order interactions have been neglected. The energy spectra of the fields ϕ_{\pm} are easily obtained. The energy ω of the charged vector field $\phi_{\pm} \propto e^{i\omega t}$ is given by $\omega^2 = k_3^2 + 2gB(n + 1/2) \pm 2gB$. Integer $n \geq 0$ denote Landau levels and k_3 does momentum parallel to the magnetic field.

The term $\pm 2gB$ in ω^2 comes from the non-minimal interaction which represents anomalous magnetic moment of the charged vector fields. It is obvious that the modes of ϕ_+ have imaginary frequencies $\omega^2 = k_3^2 - gB < 0$ when $n = 0$ and $k_3^2 < gB$. The modes occupy the lowest Landau level ($n = 0$). This implies that the field ϕ_+ increase exponentially in time. The modes with $\omega^2 < 0$ are called as Nielsen-Olesen unstable modes. Therefore, when homogeneous color magnetic fields are present, the states are unstable; the Nielsen-Olesen unstable modes are generated spontaneously and the states decay into more stable states. This is the Nielsen-Olesen instability in the gauge theory.

For the convenience of later discussions, we write down the Hamiltonian¹⁷⁾ of the field ϕ_+ neglecting higher order interactions,

$$H = |\partial_t \phi_+|^2 + |\vec{D}\phi_+|^2 - 2gB|\phi_+|^2, \quad (3)$$

where the term $|\vec{D}\phi_+|^2$ becomes $(k_3^2 + gB)|\phi_+|^2$ when ϕ_+ occupies the lowest Landau level under the homogeneous color magnetic field B . The Hamiltonian holds even for inhomogeneous magnetic field $B = \epsilon_{i,j} \partial_i A_j$. We can see that even when inhomogeneous magnetic field B is present, the presence of the field ϕ_+ can make lower the energy than the energy ($= 0$) of the state with $\phi_+ = 0$. In the sense, inhomogeneous magnetic fields are also unstable in general. (In order to demonstrate the instability we need to show the presence of bound state solutions by solving eq(4) in the next section.) We call the field ϕ_+ as Nielsen-Olesen field. Similarly, the field ϕ_- is a Nielsen-Olesen field for the inhomogeneous B since it also describes unstable modes; the Hamiltonian of ϕ_- is given by $H(\phi_-) = |\partial_t \phi_-|^2 + |\vec{D}\phi_-|^2 + 2gB|\phi_-|^2$ and the sign of gB can be negative in the transverse space.

§4. Our assumption for analysis of instability in gauge fields

First of all, we explain assumptions used in our simple model for gauge field evolution in heavy ion collisions. Here we use the Cartesian coordinate for the explanation. Initial gauge fields independent of the rapidity used in our model are only longitudinal color electric and magnetic fields. They are maximal Abelian components of gauge fields. For example, $A_i^a = (0, 0, A_i^3)$ in the SU(2) gauge theory. Then, non-Abelian interactions vanish and only linear equations remain. It has been discussed¹⁴⁾ that even if we make such a simplification of initial gauge fields in the glasma, we can reproduce quite well the numerical results⁵⁾ in their evolution at least

for $\tau > Q_s^{-1}$. Thus, the approximate use of such Abelian initial gauge fields instead of the non-Abelian glasma is appropriate. This is the first our assumption.

Such Abelian gauge fields are inhomogeneous in transverse space similarly as the glasma. Then, as we have discussed in eq(3), the color magnetic fields B are unstable energetically owing to the presence of Nielsen-Olesen fields. This instability represents instability of the glasma in our model. It is described by the equation,

$$\omega^2 \phi = (-D_T^2 + k_3^2 - 2gB)\phi \quad (4)$$

with $D_T^2 = (\vec{\partial}_T + ig\vec{A}_T)^2$ and $B = \text{rot}A_T$, where we assume that $\phi \propto \exp(i\omega t - ik_3 x_3)$. The equation can be derived from the Hamiltonian in eq(3). It is a "Schrödinger equation" of charged particles under the magnetic field B with an additional potential term $-2gB$. There are solutions of "bound states". The binding energy is given by $-\omega^2 > 0$. Thus, the growth rate of the unstable modes is given by the imaginary part of the frequency ω .

The second our approximation is to replace inhomogeneous B in the operator, $-\vec{D}_T^2 - 2gB$ in eq(4) with effective homogeneous one \bar{B} , keeping the eigenvalue of the operator $-\vec{D}_T^2 - 2gB$ unchanged. We should note that the dependence of the longitudinal momentum k_3 in the growth rate and the momentum distribution $\phi(k_3)$ do not change even if we make the replacement as far as eigenvalues of the operator, $-D_T^2 - 2gB$, are the same.

Thus, by the replacement we can analyze what we are concerned with, that is, the time evolutions of the unstable modes and the characteristic features, e.g. growth rates, associated with the evolutions. But local behaviors of the fields in the transverse space are lost by the replacement. The replacement is possible in principle, but is difficult in practice. In our simple model, the value of \bar{B} is determined by comparing our results with the previous simulation.⁹⁾

§5. Our simple model of Nielsen-Olesen instability in glasma

Now we explain the detail of our simple mode for the glasma decay. We use the proper time coordinate, $\tau = \sqrt{x_0^2 - x_3^2}$ and rapidity, $\eta = \log(\frac{x_0 + x_3}{x_0 - x_3})$, as a longitudinal coordinate. The coordinate is convenient for the description of expanding "glasma" generated in the early stage of heavy ion collisions. The collisions occur at $x_3 = 0$ ($\eta = 0$) and $x_0 = 0$ ($\tau = 0$) in extremely high energies. Thus, the heavy ions are Lorentz contracted to have vanishing width in the longitudinal direction and only extended in the transverse directions with coordinates $x_i = (x_1, x_2)$.

We analyze SU(2) gauge fields, \vec{A}_μ . Corresponding gauge fields in the coordinates are given such as \vec{A}_τ , \vec{A}_η and $\vec{A}_i = (\vec{A}_1, \vec{A}_2)$. Taking a gauge condition, $\vec{A}_\tau = 0$, the Lagrangian of the fields is given by

$$\tau L = \tau \left(\frac{1}{2\tau^2} (\partial_\tau \vec{A}_\eta)^2 + \frac{1}{2} (\partial_\tau \vec{A}_i)^2 - \frac{1}{2\tau^2} \vec{F}_{\eta,i}^2 - \frac{1}{4} \vec{F}_{i,j}^2 \right), \quad (5)$$

with $\vec{F}_{\eta,i}^2 = (\partial_\eta \vec{A}_i - \partial_i \vec{A}_\eta + g\vec{A}_\eta \times \vec{A}_i)^2$ and $\vec{F}_{i,j}^2 = (\partial_i \vec{A}_j - \partial_j \vec{A}_i + g\vec{A}_i \times \vec{A}_j)^2$.

We define the complex fields, ϕ_η , ϕ_i , and real ones, A_η , A_i by rearranging color components of the gauge fields,

$$\vec{A}_\eta = (A_\eta^1, A_\eta^2, A_\eta^3) = \left(\frac{\phi_\eta + \phi_\eta^\dagger}{\sqrt{2}}, \frac{\phi_\eta - \phi_\eta^\dagger}{i\sqrt{2}}, A_\eta \right) \quad \text{and} \quad \vec{A}_i = \left(\frac{\phi_i + \phi_i^\dagger}{\sqrt{2}}, \frac{\phi_i - \phi_i^\dagger}{i\sqrt{2}}, A_i \right), \quad (6)$$

and define the following "charged field" with spin parallel, ϕ_+ (anti-parallel, ϕ_- ,) to the longitudinal direction, $\phi_\pm \equiv \frac{\phi_{1\pm} + i\phi_2}{\sqrt{2}}$. Initial gauge fields are introduced as maximal Abelian component A_η, A_i of the gauge fields as we mentioned above. It is easy to see that the fields, ϕ_η and ϕ_\pm , are transformed under the gauge transformation, $A_\mu \rightarrow U^\dagger A_\mu U + g^{-1} U^\dagger \partial_\mu U$ with $U = \exp(i\theta\sigma_3)$, such that $\phi_{\eta,\pm} \rightarrow \exp(-i\theta)\phi_{\eta,\pm}$, where σ_i are Pauli matrices and θ is a constant independent of τ . Therefore, we may think that the complex fields, $\phi_{\eta,\pm}$ are U(1) charged fields corresponding to the symmetry.

We introduce a longitudinal color magnetic field B and an color electric field E as initial background gauge fields, both of which are assumed to point to the third direction in SU(2) gauge group; $B = \epsilon_{i,j}\partial_i A_j$ and $E = \frac{1}{\tau}\partial_\tau A_\eta$. The fields point to the direction parallel to the collision axis in the real space; $\vec{B} = (0, 0, B)$ and $\vec{E} = (0, 0, E)$. We assume that the background fields are generated at $\tau = 0$ in heavy ion collisions.

With the use of the fields, $A_{i,\eta}$ and $\phi_{\pm,\eta}$, the Lagrangian leads to

$$\begin{aligned} \tau L = & \frac{\tau}{2}(\partial_\tau A_i)^2 + \frac{1}{2\tau}(\partial_\tau A_\eta)^2 + \tau(|\partial_\tau \phi_+|^2 + |\partial_\tau \phi_-|^2) + \frac{1}{\tau}|\partial_\tau \phi_\eta|^2 - \frac{\tau}{4}f_{i,j}^2 - \frac{1}{2\tau}f_{\eta,i}^2 \\ & - \tau(|D_i \phi_+|^2 + |D_i \phi_-|^2) - \frac{1}{\tau}(|D_\eta \phi_+|^2 + |D_\eta \phi_-|^2 + |D_i \phi_\eta|^2) + 2\tau g B(|\phi_+|^2 - |\phi_-|^2) \\ & + \frac{\tau}{2}|D_- \phi_+ + D_+ \phi_-|^2 + \frac{1}{\sqrt{2}\tau}((D_- \phi_+ + D_+ \phi_-)D_\eta \phi_\eta + c.c.) + \\ & \left(\frac{2gi}{\sqrt{2}\tau}(f_\eta \phi_+ + f_\eta^\dagger \phi_-)\phi_\eta^\dagger + c.c. \right) - \frac{g^2}{\tau}|\phi_\eta \phi_+^\dagger - \phi_\eta^\dagger \phi_-|^2 - \frac{\tau g^2}{2}(|\phi_+|^2 - |\phi_-|^2)^2, \quad (7) \end{aligned}$$

with $f_{i,j} \equiv \partial_i A_j - \partial_j A_i$, $f_{\eta,i} \equiv \partial_\eta A_i - \partial_i A_\eta$, $f_\eta \equiv f_{\eta,1} - if_{\eta,2}$, $D_i \equiv \partial_i + igA_i$, $D_\eta \equiv \partial_\eta + igA_\eta$, and $D_\pm \equiv D_1 \pm iD_2$, where we have neglected surface terms just like $\partial_i J_i$.

Obviously, the Lagrangian is invariant under the U(1) gauge transformation, $\phi_{\pm,\eta} \rightarrow \phi_{\pm,\eta} \exp(-i\theta)$ along with $A_{i,\eta} \rightarrow A_{i,\eta} + g^{-1}\partial_{i,\eta}\theta$. The kinetic energies of the fields A_i , A_η , ϕ_\pm and ϕ_η , are presented in the first line of the Lagrangian. In the second line, minimal interactions between $\phi_{\pm,\eta}$ and the abelian gauge fields, A_i and A_η are presented. We can see in the second line that the charged fields ϕ_\pm receive anomalous magnetic moments, $2\tau g B(|\phi_+|^2 - |\phi_-|^2)$. This term plays an important role for making the field ϕ_+ unstable, that is, Nielsen-Olesen unstable mode. There are the quartic interactions of the fields in the fourth line, which describe repulsive forces among the fields $\phi_{\eta,\pm}$. The repulsive force leads to the saturation of the exponential increase observed in the simulation.⁹⁾ The terms in the third line are

irrelevant to our discussion below (the terms can be gauged away).

When an initial gauge field configuration of $B = \epsilon_{i,j} \partial_i A_j$ and $E = \frac{1}{\tau} \partial_\tau A_\eta$ is given at $\tau = 0$, the subsequent evolution of the fields A_η and A_i is governed by the equations,

$$\begin{aligned} \partial_\tau \left(\frac{1}{\tau} \partial_\tau A_\eta \right) - \frac{1}{\tau} (\partial_i^2 A_\eta - \partial_\eta \partial_i A_i) &= 0, \\ \text{and } \partial_\tau (\tau \partial_\tau A_i) - \tau (\partial_j^2 A_i - \partial_i \partial_j A_j) + (\partial_\eta^2 A_i - \partial_i \partial_\eta A_\eta) &= 0. \end{aligned} \quad (8)$$

The equations are obtained from the Lagrangian by neglecting the other charged fields. The approximation is valid when the other fields are sufficiently small so that the interactions between E , B and the others can be neglected. A solution of B and A_η independent of the rapidity η is given by $B = B_0 J_0(Q_0 \tau) \cos(\vec{Q}_0 \vec{x})$ and $A_\eta = c \tau J_1(Q_0 \tau) \cos(\vec{Q}_0 \vec{x})$, where we suppose that the fields carry a transverse momentum, \vec{Q}_0 ($Q_0 = |\vec{Q}_0|$) as a typical transverse momentum of background gauge fields. B_0 is a constant and $J_{0,1}(Q_0 \tau)$ are Bessel functions. (General solutions are given by the average in Q_0 over momentum distributions.) A constant of c may be determined by the requirement that $B = E$ as $\tau \rightarrow 0$. It leads to $c = B_0/Q_0$. The requirement arises from the initial condition of $\langle \text{Tr}(B^2) \rangle = \langle \text{Tr}(E^2) \rangle$ for $\tau \rightarrow 0$ given in the MV model of CGC.¹⁸⁾ Here, the expectation of $\langle \sim \rangle$ is taken over the distribution of large x gluons according to the MV model.

Here we neglect spatial dependence of the gauge fields according to the second our assumption. Additionally we simplify the factor $J_0(Q_0 \tau)$ such that $J_0(Q_0 \tau) \rightarrow \sin(Q_0 \tau) \sqrt{2/\pi Q_0 \tau} \sim \sqrt{2/\pi Q_0 \tau}$ by neglecting the oscillating factor $\sin(Q_0 \tau)$. This smooth decay of the fields roughly coincides with the numerical evolutions of the glasma.⁵⁾ Hence, the simplification is appropriate for discussing small fluctuations around the slowly decaying background gauge fields. Therefore, we assume the following background initial gauge fields,

$$B = B_0 \sqrt{2/\pi Q_0 \tau} \quad \text{and} \quad A_\eta = B_0 (\tau/Q_0) \sqrt{2/\pi Q_0 \tau}, \quad (9)$$

which reproduce the smooth decay of $\langle \text{Tr}(B^2) \rangle$ and $\langle \text{Tr}(E^2) \rangle$ for large τ .

Under the background gauge fields, we analyze the development of the small fluctuations $\phi_{\eta,\pm}$. The fluctuations correspond to the small fluctuations added to initial background gauge fields in the previous simulation.⁹⁾ Since they are supposed to be much small, we take into account only quadratic terms of the fields in the Lagrangian. These fluctuations in general oscillate with small amplitudes. But one of these fluctuations increases exponentially. In our model the field ϕ_+ (or ϕ_- when $gB < 0$) is the one increasing exponentially with τ . The other fields simply oscillate and their amplitudes remain small.

We write down the equation of motion of the field ϕ_+ ,

$$\partial_\tau^2 \phi_+ + \frac{1}{\tau} \partial_\tau \phi_+ + \left(\frac{(k_\eta - gA_\eta(\tau))^2}{\tau^2} - gB(\tau) \right) \phi_+ = 0, \quad (10)$$

where k_η denotes a longitudinal momentum; $\phi_+ \propto \exp(-ik_\eta \eta)$. We have taken only a component in the lowest Landau level. It is easy to see that due to the last term

$-gB(\tau)$, ϕ_+ increases exponentially just as $\phi_+ \propto \exp(\sqrt{gB}\tau)$ for $\tau \rightarrow \infty$ when gB is independent of τ , i.e. a solution of the equation, $\partial_\tau^2 \phi_+ - gB\phi_+ \simeq 0$. Their wave functions are given such that $\phi_+ = g_m(\tau)z^m \exp(-|\vec{x}'|^2/4l_B^2)$ with $z = x_1 + ix_2$ and integers, $m \geq 0$, where $l_B = 1/\sqrt{gB}$ denotes cyclotron radius and $g_m(\tau)$ is governed by the eq(10); we have neglected the smooth expansion of the cyclotron radius.

§6. Our results

In order to solve the eq(10) with $A_\eta(\tau)$ and $B(\tau)$ given in eq(9), we rewrite the equation in the following,

$$\partial_{\tau'}^2 \phi_+ + \frac{1}{\tau'} \partial_{\tau'} \phi_+ + \left(\frac{(k_\eta - b\sqrt{\tau'})^2}{\tau'^2} - \frac{a}{\sqrt{\tau'}} \right) \phi_+ = 0, \quad (11)$$

where dimensionless parameters are defined as $\tau' \equiv Q_s \tau$, $a \equiv \sqrt{2/\pi}(gB_0/Q_0^2) \times (Q_0/Q_s)^{3/2}$ and $b \equiv \sqrt{2/\pi}(gB_0/Q_0^2) \times (Q_0/Q_s)^{1/2}$. In the subsequent calculations we treat the scale of the field ϕ_+ arbitrary although it is much smaller than the background field. This is allowed in the approximation of taking only quadratic terms of the field ϕ_+ in the Lagrangian. The coefficients a and b are determined for reproducing the results in the previous simulation;⁹⁾ actually we have used $a = (0.05)^2$ and $b = 0.38$ in order to obtain our curve in Fig.5.

Before solving the equation (11) numerically, we briefly explain how the solutions behave with τ' . The term of $\left(\frac{(k_\eta - b\sqrt{\tau'})^2}{\tau'^2} - \frac{a}{\sqrt{\tau'}} \right)$ ($\equiv \omega_s^2$) is just a spring constant. The term of $\frac{1}{\tau'} \partial_{\tau'} \phi_+$ represents a friction, which becomes weaker as τ' becomes larger. Thus, we understand that the field oscillates as far as $\omega_s^2 > 0$, that is, in the early stage ($\tau' \sim O(1)$) after the production of the background fields. The spring constant ω_s^2 becomes small with τ' . Once ω_s^2 becomes negative, the field stops the oscillation and begins to increase exponentially.

In Fig.1 we show the typical behavior of the field, $\phi_+(k_\eta = 16.5, \tau')$, with the initial conditions of $\phi_+(\tau' = 0.01) = 1$ and $\partial_\tau \phi_+(\tau' = 0.01) = 0$. (Obviously, taking different initial conditions do not change the global behavior of ϕ_+ for large τ' , since it simply oscillates in small τ' .) The field increases exponentially after the oscillation in the early stage. When the longitudinal momentum k_η becomes large, the time τ when the field $\phi_+(k_\eta, \tau')$ begins to increase exponentially, becomes large. This implies that as τ' becomes larger, the modes with larger longitudinal momentums are excited.

In Fig.2 we show the time dependence of the maximal momentum $k_\eta(\max)$. The maximal momentum $k_\eta(\max)$ at the time τ' is defined as the momentum with which the mode $\phi_+(k_\eta(\max), \tau')$ starts to increase exponentially at the time τ' . The modes with $k_\eta < k_\eta(\max)$ have already been increasing exponentially at the time τ' . The maximal momentum $k_\eta(\max)$ may be obtained by solving the condition of the spring constant $\omega_s^2 = 0$, but $k_\eta(\max)$ is defined as $|\phi_+(k_\eta(\max), \tau')| = 2$ in our calculation. We have shown both results in Fig.2, which almost coincide with each other. $k_\eta(\max)$ increases almost linearly in τ' , but the solution of $\omega_s^2 = 0$

shows that $k_\eta(\text{max}) \propto \tau'^{3/4}$. The result agrees with the previous one,⁹⁾ although the rate of the increase is approximately four times smaller than the previous one; $k_\eta(\text{max}) \simeq 0.015 Q_s \tau + 5$.

It has been shown⁹⁾ that $k_\eta(\text{max})$ deviates from the linear dependence around the time when the exponential increase is saturated. After the deviation, $k_\eta(\text{max})$ increases very rapidly. These phenomena could be understood in our model as the result due to the onset of quartic interactions among the field ϕ_+ . The quartic interactions make the energy of the mode with largest amplitude be transmitted to the other modes with higher longitudinal momenta.

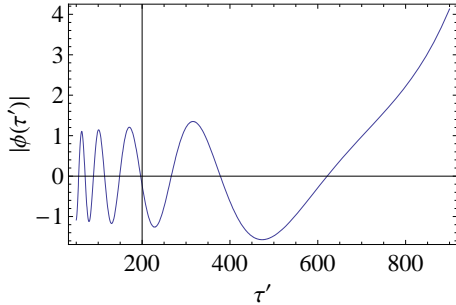


Fig. 1. After the oscillation, $\phi_+(k_\eta = 16.5)$ increases exponentially with $\tau' = Q_s \tau$.

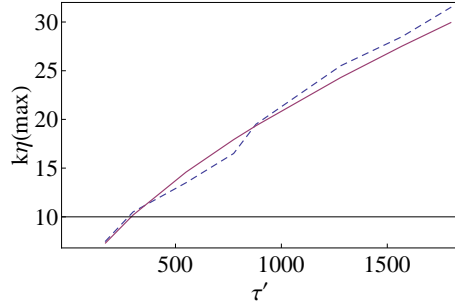


Fig. 2. solution of $\omega_s^2 = 0$ (solid), $k_\eta(\text{max})$ (dashing) increases almost linearly with $\tau' = Q_s \tau$.

Before proceed to make the comparison, we should mention why we compare the evolution of the field ϕ_+ with the evolution of longitudinal pressure discussed in the previous simulation.⁹⁾ Their behaviors are quite similar to each other. Roughly speaking, there are two components of fields involved in the ref.,⁹⁾ large ones and much small ones. The large ones $A(\text{large})$ are just the background fields independent of rapidity, which are produced according to the MV model. On the other hand, the small ones $a(\text{small})$ are fluctuations depending on the rapidity which are added by hand to the background fields. In the circumstance, the longitudinal pressure P_η is composed of two parts, $P_{\eta,0}$ and δP_η ; $P_\eta = P_{\eta,0} + \delta P_\eta$.

$$P_\eta = \tau^{-2} \left(\vec{F}_{\eta,i}^2 + (\tau \partial_\tau \vec{A}_i)^2 \right) - \vec{F}_{1,2}^2 - \left(\frac{1}{\tau} \partial_\tau \vec{A}_\eta \right)^2 \simeq P_{\eta,0} + \delta P_\eta, \quad (12)$$

where $P_{\eta,0}$ is rapidity independent and is formed only of the large components, while δP_η is formed of the small components as well as the large ones; $\delta P_\eta = P(A(\text{large})) \times a(\text{small})$. The linear dependence on $a(\text{small})$ comes from the approximation of $a(\text{small}) \ll A(\text{large})$. $P_{\eta,0}$ decreases smoothly with τ . On the other hand, δP_η increases exponentially although it is still much smaller than $P_{\eta,0}$. Therefore, some of small components $a(\text{small})$ depending on the rapidity, increase exponentially as has been shown.⁹⁾ Our simple model of gauge field evolution indicates that such a small component is just the Nielsen-Olesen unstable mode ϕ_+ . That is the reason why we compare the evolution of the field ϕ_+ with the evolution of the longitudinal pressure. It should be noted that the Fourier component of δP_η in the rapidity is

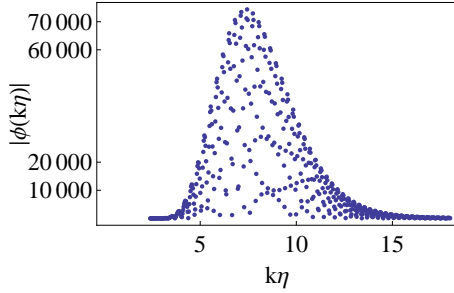


Fig. 3. distribution of longitudinal momentum k_η at $\tau' = Q_s\tau = 1500$.

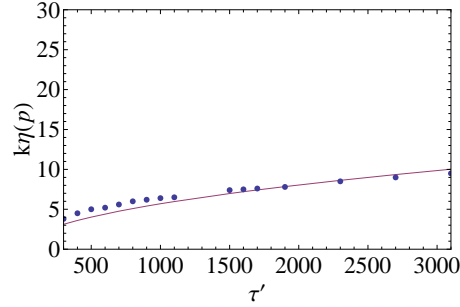


Fig. 4. τ' dependence of $k_\eta(p)$ (dot) and $k_\eta = 0.18\sqrt{\tau'}$ (solid).

determined only by the factor of a (small), which corresponds to small fluctuations $\phi_{\eta,\pm}$ in our model.

We now proceed to make the further comparison. In Fig.3, we show the typical momentum distribution $|\phi_+(k_\eta, \tau')|$ at $\tau' = 1500$. The distribution in k_η has been obtained by solving eq(11) for $\phi_+(k_\eta, \tau')$ with each k_η chosen within the range $0.24 \leq k_\eta \leq 18$ by $\delta k_\eta = 0.03$. The distribution is not smooth but oscillating rapidly in k_η . (When we magnify a small region, e.g. $\delta k_\eta \sim 0.2$ of the Fig.3, we can see explicitly the oscillation in k_η . Roughly speaking, this oscillation comes from the oscillation of a modified Bessel function $I_{k_\eta}(Q_s\tau)$.) But we can find out a smooth distribution obtained by averaging the original one over an appropriately small but sufficiently large δk_η to be compared with wave length in the oscillation. Then, the smooth one coincides almost with the mountain-like form of the distribution in Fig.3. (The average corresponds to an average over initial conditions for solving eq(11). This is because slightly different initial conditions lead to slightly different curves.) We find that the distribution has a peak at a momentum $k_\eta(p)$. The mode with the momentum is generated most efficiently.

In Fig.4, we show how $k_\eta(p)$ depends on the time τ' ; $k_\eta(p)$ increases very slowly with τ' just as $0.18\sqrt{\tau'}$. Furthermore, we can see that the momenta are smaller than $k_\eta(\text{max})$. These results agree with the previous ones.⁹⁾ The presence of the longitudinal momentum $k_\eta(p) \simeq 6 \sim 8$ almost independent of time implies that in the decay of the gauge fields uniform in η , specific modes with the momentum $k_\eta(p)$ is generated most efficiently, which breaks the homogeneity in η . We do not understand why such specific momenta are present.

Finally, we show in Fig.5 how $|\phi_+(k_\eta(p), \tau)|$ increases with τ' , that is, the time dependence of the peak $|\phi_+(k_\eta(p), \tau)|$. It increases as $\exp(\tau'^{3/4})$ for $\tau' \rightarrow \infty$, which can be read from the equation(11). The growth rate is defined as $(\log |\phi|)/\tau$. Thus, the growth rate of the field $|\phi_+(k_\eta(p), \tau)|$ decreases slowly with τ . Since $k_\eta(p)$ is almost constant in time, $|\phi_+(k_\eta, \tau)|$ also increases in the similar way to $|\pi_+(k_\eta(p), \tau)|$ for any k_η .

For a comparison, we have depicted the Fourier component of the longitudinal pressure, $P_\eta(k_\eta(p)) = (d_0 + d_1 \exp(0.427\sqrt{\tau'}))$ in the ref.⁹⁾ as well as the function of $\exp(0.00544\tau')$ also used in the ref.⁹⁾ Obviously, the field, $|\phi_+(k_\eta(p), \tau')|$, in

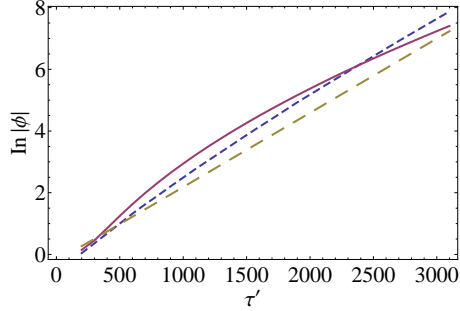


Fig. 5. longitudinal pressure $P_\eta(k_\eta(p))$ (solid) in ref.⁹⁾, $|\phi_+|$ (short dashed) and $\exp(0.00544\tau')$ (dashed).

our calculation agrees with the longitudinal pressure better than the function of $\exp(0.00544\tau')$. (In Fig.5, we take the scale arbitrary in the vertical coordinate. In order for $|\phi_+(k_\eta(p), \tau')|$ to coincide precisely with the pressure shown in the ref.,⁹⁾ we have only to take the scale of the field $|\phi_+(k_\eta(p), \tau')|$ appropriately.) Our simulation does not reproduce strictly the behavior of the pressure such as $\exp(\sqrt{\tau'})$. We expect that the more elaborate treatment of the background magnetic field may give rise to the behavior $\exp(\sqrt{\tau'})$. (When B decreases as $\sim 1/\tau'$ instead of $1/\sqrt{\tau'}$, this behavior can be obtained. We will discuss the validity of the behavior $B \sim 1/\tau'$ in near future.)

As it has been shown, the behaviors of the longitudinal pressure calculated in the MV model with the small fluctuations added can be roughly reproduced in our simple model: 1) $k_\eta(\text{max})$ increases linearly with τ , 2) $k_\eta(p)$ depends on τ very weakly and $k_\eta(p)$ is much smaller than $k_\eta(\text{max})$, and 3) the pressure $P_\eta(k(p))$ increases with τ as $\exp(\tau^{3/4})$, although the pressure obtained in the simulation increase as $\exp(\sqrt{\tau})$. Furthermore, we may argue that the saturation of the exponential increase arises due to the repulsive self-interaction of ϕ_+ in our model. The repulsive interaction need more energies for the field to increase more. Thus, it would stop the field increasing. Although our results are different in detail with those in the simulation, the rough agreement shows that our simple model of instabilities is valid approximation for the instabilities observed in the glasma. Thus, the instabilities of the glasma observed in the previous simulation is caused by the Nielsen-Olesen unstable mode.

In order to obtain these results, we have used the parameters such as $a = (0.05)^2$ and $b = 0.38$. Roughly speaking, the parameter a gives the growth rate of the field ϕ_+ . Thus, the parameter can be determined by making it fit the growth rate obtained in the simulation.⁹⁾ But the growth rate shown in the simulation is the one of the field $\phi_+(k_\eta(p))$, not $\phi_+(k_\eta)$ itself. Here $k_\eta(p)$ depends on τ although the dependence is very weak. This requires a careful adjustment of the other parameter b .

The determination of the parameters in detail is not important. An important thing is that these parameters lead to a weak homogeneous color magnetic field B_0 . Actually, the above values of a and b corresponds to the physical parameters of $Q_0 \simeq Q_s/152$ and $gB_0 \simeq 4.7Q_0^2$. Thus, the growth rate $\sim \sqrt{gB_0}$ discussed in the

section (4) is much smaller than $\sqrt{g|B|} \sim Q_s$. Indeed, the growth rate is about $0.00544Q_s$ derived from the reference function $\exp(0.00544\tau')$ depicted in Fig.5.

We should mention that the smallness of the growth rate comes from the inhomogeneity of the glasma. The potential $-2gB \sim Q_s^2$ for the field ϕ_+ in eq(4) varies so rapidly in transverse space; it has many attractive regions ($-2gB < 0$) and repulsive regions ($-2gB > 0$) whose widths are of the order Q_s^{-1} . Wave functions of the bound states are extended over these regions involving both attractive and repulsive potentials; they can never be trapped within a region with attractive potential. Therefore, the binding energies $-\omega^2$ become much smaller than Q_s^2 . Thus, the growth rate becomes much smaller than Q_s .

§7. Conclusion

To summarize, we have discussed that inhomogeneous color magnetic fields $gB \sim Q_s^2$ produced in the high energy heavy ion collisions decay with the production of the Nielsen-Olesen fields ϕ_+ . Instead of analyzing the evolution of the field ϕ_+ under the inhomogeneous color magnetic fields, we analyze it using an effective homogeneous color magnetic field. Then, we have compared the time evolution of the Nielsen-Olesen field ϕ_+ with the evolution of the longitudinal pressure shown in the simulation.⁹⁾ We have found that our simple model with the effective weak homogeneous color magnetic field gB_0 reproduces the important features clarified in the simulation; growth rates, longitudinal momentum distributions, etc. of the unstable modes. The coincidence is not accidental. These are properties associated with time and longitudinal directions. Even if we use the homogeneous magnetic field, the properties of the unstable modes can be reproduced in principle. On the other hand, properties associated with the transverse directions can not be reproduced with the use of such fields. Therefore, our analysis shows that the decay of the glasma generated initially at $\tau = 0$ in heavy ion collisions is caused by Nielsen-Olesen instability.

On the other hand, there is an insistence^{9),19)} that Weibel instability known in plasma physics is the cause of the glasma instability: Inhomogeneous electromagnetic plasma whose momentum distribution depends only on transverse momentum, shows Weibel instability under small magnetic field applied. The instability is discussed by using the Boltzmann equation of charged (color charged) particles coupled with electromagnetic (color gauge) fields, while the glasma instability in the simulation has been shown in pure gauge theory. Nielsen-Olesen instability is the instability arising in pure gauge theory. In this sense, the relevance of the Weibel instability to the glasma instability is not obvious. Thus, it is reasonable to think that the glasma instability shown in the simulation is just Nielsen-Olesen instability. We will discuss in future publications why the glasma instability is just Nielsen-Olesen instability, not Weibel one.

We would like to express thanks to Dr.K. Itakura in KEK and Dr.H. Fujii in University of Tokyo for useful comments.

References

- 1) L.D. McLerran and R. Venugopalan, Phys. Rev. D49, 2233 (1994); D49, 3352 (1994); D50, 2225 (1994).
- 2) A. Krasnitz and R. Venugopalan, Nucl. Phys. B557, 237 (1999); Phys. Rev. Lett. 84, 4309 (2000); 86, 1717 (2001).
- 3) A. Krasnitz, Y. Nara and R. Venugopalan, Phys. Rev. Lett. 87, 192302 (2001); Nucl. Phys. A717, 268 (2003).
- 4) T. Lappi, Phys. Rev. C67, 054903 (2003); C70, 054905.
- 5) T. Lappi and L. McLerran, Nucl. Phys. A772, 200 (2006).
- 6) E. Iancu, A. Leonidov and L. McLerran, hep-ph/0202270.
E. Iancu and R. Venugopalan, hep-ph/0303204.
- 7) T. Hirano and Y. Nara, Nucl. Phys. A743, 305 (2004); J. Phys. G30, S1139 (2004).
- 8) A. Iwazaki, Phys. Rev. C77, 034907 (2008).
- 9) P. Romatschke and R. Venugopalan, Phys. Rev. Lett. 96, 062302 (2006); Phys. Rev. D74, 045011 (2006).
- 10) K. Fukushima, F. Gelis and L. McLerran, Nucl. Phys. A786, 107 (2006).
- 11) F. Gelis, T. Lappi and R. Venugopalan, hep-ph/0708.0047.
- 12) N.K. Nielsen and P. Olesen, Nucl. Phys. B 144 (1978) 376; Phys. Lett. B 79 (1978) 304.
- 13) G.K. Savvidy, Phys. Lett. B 71 (1977) 133.
H. Pagels, Lecture at Coral Gables, Florida, 1978.
- 14) Y.V. Kovchegov, Nucl. Phys. A762 298 (2005).
T. Lappi, Phys. Lett. B643 11 (2006).
H. Fujii and K. Itakura, Nucl. Phys. A809 88 (2008).
H. Fujii, K. Fukushima and Y. Hidaka, hep-ph/0811.0437.
- 15) M. Gyulassy and A. Iwazaki, Phys. Lett. 165B 157 (1985).
N. Tanji, hep-ph/08104429, see references in the paper.
- 16) Z.F. Ezawa and A. Iwazaki, Phys. Rev. D25 2681 (1982).
- 17) A. Iwazaki, Phys. Rev. D75:034020 (2007).
- 18) K. Fukushima, Phys. Rev. C76, 021902(R) (2007).
- 19) P. Arnold and G.D. Moore, Phys.Rev. D76:045009 (2007).